Fast and Accurate Language Model Decoding via Parallel Token Processing

Zhepei Wei Wei-Lin Chen Xinyu Zhu Yu Meng
Department of Computer Science
University of Virginia
`{zhepei.wei,wlchen,xinyuzhu,yumeng5}@virginia.edu`

Abstract

Autoregressive decoding suffers from an inherent efficiency bottleneck due to its sequential token generation process, where each token must be generated before the next can be processed. This sequential dependency significantly limits the ability to fully exploit the parallel processing power of modern hardware. While speculative decoding and layer skipping offer promising speedups, both approaches come with drawbacks. Speculative decoding relies on a secondary small "drafter" model, which not only increases memory overhead but may also be unavailable in many cases—the drafter must share the same tokenizer and vocabulary as the main model for compatibility between generated and verified tokens. Layer skipping, on the other hand, can cause discrepancies in the generated output compared to standard autoregressive decoding, as skipped layers do not compute the key-value (KV) cache that plays a crucial role in predicting future tokens. In this work, we introduce a fast and accurate decoding method, ParaDecode, which accelerates autoregressive decoding while ensuring output parity, without the need for auxiliary models or changes to original model parameters. Our approach is driven by the observation that many tokens—particularly simple or highly-predictable ones—can be accurately predicted using intermediate layer representations, without requiring computation through the entire model. Once the model reaches a certain confidence, further layers are unlikely to significantly alter the prediction. ParaDecode generates tokens at an intermediate layer when confidence is sufficiently high. This allows the next token computation to start immediately, in parallel with the completion of the KV cache computation for the early-predicted token in its remaining layers. This parallelism, implemented using batched matrix operations, enables simultaneous processing of multiple tokens across different layers, thereby maximizing hardware utilization and reducing overall decoding latency. To ensure output consistency, a final verification step is applied to guarantee that the early-predicted tokens match the results of standard autoregressive decoding. Experiments show that ParaDecode achieves up to **1.53**$\times$ speedup across various generation tasks.

1 Introduction

The autoregressive decoding process in large language models (LLMs) is increasingly becoming a critical efficiency bottleneck for text generation [34]. As each token generation depends on previously generated ones, the inherently sequential nature of this process severely limits parallelization capabilities on modern hardware [41]. This challenge is becoming more pressing due to two key trends. Firstly, LLMs continue to grow exponentially in size [33, 24, 14, 1, 56, 18, 31, 2], resulting in substantially more time-consuming and resource-intensive computations at each step of token generation. Secondly, model-generated outputs are becoming progressively longer [44, 50, 7, 46, 6], which require massive inference steps. The confluence of these factors leads to significant latency in text generation, amplifying the urgent need for more efficient decoding methods.

AFM Workshop at 38th Conference on Neural Information Processing Systems (NeurIPS 2024).

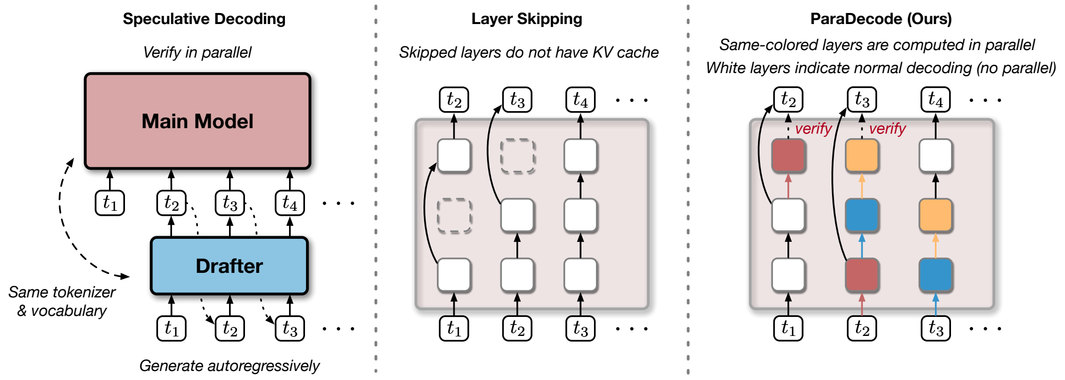
Speculative Decoding
Verify in parallel
Main Model
Drafter
Same tokenizer & vocabulary
Generate autoregressively
Layer Skipping
Skipped layers do not have KV cache
ParaDecode (Ours)
Same-colored layers are computed in parallel
White layers indicate normal decoding (no parallel)
verify
verify

Figure 1: (Left) Speculative decoding relies on an auxiliary drafter model, leading to increased memory usage and requiring the same tokenizer and vocabulary as the main model. (Middle) Layer skipping bypasses certain layers, which results in missing KV cache at those layers and can introduce discrepancies in future token predictions. (Right) ParaDecode accelerates decoding by processing tokens in parallel.

To accelerate autoregressive decoding, two primary approaches have emerged: speculative decoding and layer skipping, as illustrated in Figure 1. Speculative decoding [37, 9, 40, 42, 23, 28] employs a lightweight secondary model, called a "drafter," to generate candidate tokens at lower latency, which are then verified in parallel by the larger main model. However, the reliance on a separate drafter model increases memory overhead and can be impractical in many cases, since the drafter must share the same tokenizer and vocabulary as the main model to ensure token compatibility. Layer skipping [27, 19, 20, 15, 48, 22, 17], in contrast, reduces computation cost by selectively bypassing certain layers during token generation. This approach often requires designing new model architectures and intricate training methods [20, 48]. Although effective at reducing latency, layer skipping often leads to discrepancies in output quality compared to standard autoregressive decoding [49, 38]. Specifically, skipped layers do not compute the key-value (KV) cache, which is essential for maintaining consistency in the model's predictions of future tokens. As a result, while both speculative decoding and layer skipping provide promising speedups, they come with trade-offs that pose challenges for their widespread adoption in practice.

In this work, we propose ParaDecode, a fast and accurate decoding method designed to accelerate autoregressive decoding through parallel token processing. ParaDecode builds on the insight that many simple and predictable tokens can be accurately generated at intermediate layers, without requiring a full pass through all model layers [49]. To optimize token generation quality at intermediate layers, we introduce lightweight language model (LM) heads at intermediate layers, which are trained to minimize the KL divergence between their predictions and those of the final layer, while keeping the original model parameters frozen. Our preliminary studies show that when predictions at intermediate layers are sufficiently confident, subsequent layers are unlikely to significantly alter the output. Based on this observation, ParaDecode generates tokens from intermediate layers when confidence is high, and simultaneously initiates processing of the next token in parallel with the remaining layers' KV cache computation for the current token. This parallelism is achieved through batched matrix operations, allowing multiple tokens to be processed across different layers simultaneously, maximizing hardware utilization and improving overall decoding throughput. Once the KV cache for all layers is computed, we verify that the early-predicted token matches the standard autoregressive decoding result, ensuring consistency. Compared to speculative decoding and layer skipping, ParaDecode accelerates autoregressive decoding while maintaining output parity, without requiring auxiliary models or modifications to the original model parameters. Preliminary empirical studies demonstrate that ParaDecode achieves up to **1.53**$\times$ speedup across challenging text generation tasks.

2 Method: ParaDecode

In this section, we present our proposed method ParaDecode, as illustrated in Figure 2. The core concept is to start processing the initial layers of subsequent tokens in parallel with completing the current token's layers, thereby enhancing overall decoding throughput via parallel computation. We introduce the techniques for enabling early predictions using intermediate layer representations in Section 2.1, followed by a detailed explanation of our parallel processing approach in Section 2.2.

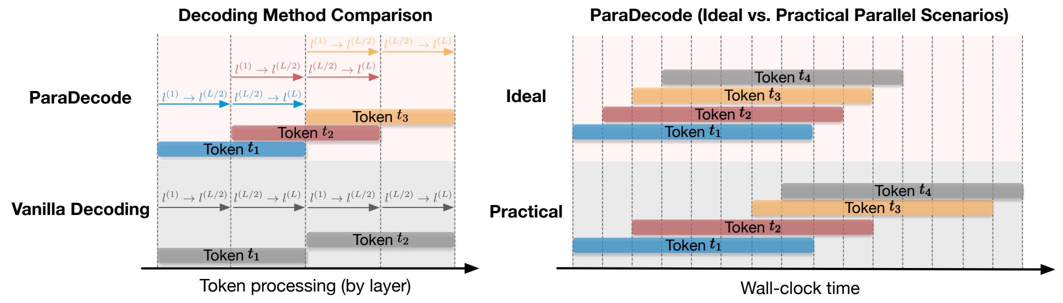
Decoding Method Comparison
ParaDecode
Vanilla Decoding
Token t_1
Token t_2
Token t_3
Token processing (by layer)
ParaDecode (Ideal vs. Practical Parallel Scenarios)
Ideal
Practical
Token t_4
Wall-clock time

Figure 2: (Left): Vanilla autoregressive decoding processes tokens strictly in sequence, limiting opportunities for parallelization. In contrast, ParaDecode starts processing the first few layers of the next token in parallel with the remaining layers of the current token, once the model can confidently predict the next token using intermediate LM heads. To illustrate, early predictions are assumed to occur at layer $L/2$, though in practice, predictions can happen at other layers based on confidence. (Right): The ideal case is shown in the upper part, where all tokens are predicted early at shallow layers, leading to maximal parallelization. The lower part shows a more typical scenario, where tokens are early predicted at different intermediate layers, resulting in varying degrees of parallelization.

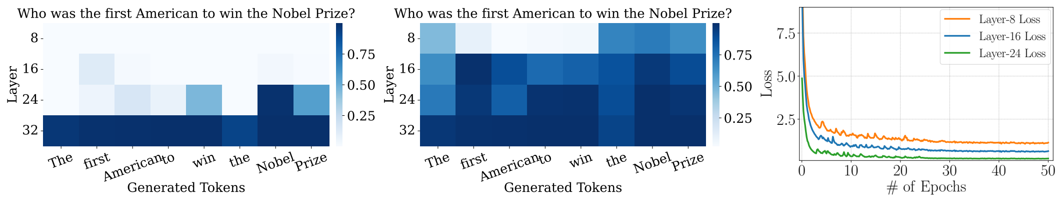

(a) w/ original LM head. (b) w/ trained LM heads. (c) KL loss curve.

Figure 3: Probabilities of model-generated tokens predicted at the 8th, 16th, 24th, and 32nd (final) layers of the fine-tuned Llama-3.1-8B-Instruct are shown using (a) the original last-layer language model (LM) head and (b) our newly introduced lightweight LM heads. These new LM heads are trained to minimize the KL divergence loss relative to the final layer predictions, while keeping all original model parameters frozen. The LM heads enable close approximation of the final predictions, as seen in (b), where many tokens have confident predictions at intermediate layers, and in (c), where the KL divergence loss relative to the final layer predictions is minimal.

2.1 Lightweight Language Model Heads Enable Early Predictions

Off-the-shelf LMs struggle with early predictions. Many tokens in natural language, such as stopwords, can be easily predicted and do not require the full capacity of a model for accurate generation. However, off-the-shelf LMs typically have difficulty utilizing intermediate layers for next-token prediction, as the final-layer LM head is not trained to work with intermediate-layer representations. As shown in Figure 3a, applying the final-layer LM head to intermediate layers results in mostly low predicted probabilities for the tokens generated by the model, making early predictions with standard LMs challenging. Hence, prior research on early exiting often involves designing specific model architectures or fine-tuning existing models to enable intermediate-layer predictions [20, 17, 15]. As a result, these acceleration methods typically fail to produce outputs consistent with those of the original off-the-shelf LMs due to changes in architecture and parameters.

Training intermediate-layer LM heads with original model parameters frozen. We hypothesize that many intermediate-layer representations may already contain sufficient information for predicting the next token, but the original LM head cannot directly harness their potential. To facilitate early predictions using intermediate-layer representations without further fine-tuning them, we introduce trainable LM heads $\boldsymbol{\theta}^{(i)} = \{\boldsymbol{e}_t^{(i)}\}_{t\in\mathcal{V}}$ at each candidate early prediction layer $l^{(i)}$. They take the hidden representations $\boldsymbol{h}^{(i)}$ at layer $l^{(i)}$ as frozen features and predict the next word distribution $p_{\boldsymbol{\theta}^{(i)}}(t|\boldsymbol{h}^{(i)})$, which are trained to approximate the last-layer prediction $p^*(t|\boldsymbol{h}^*)$ ($\boldsymbol{h}^*$ is the last-layer hidden states) by minimizing the following KL divergence loss:

$$p_{\boldsymbol{\theta}^{(i)}}(t|\boldsymbol{h}^{(i)}) = \frac{\exp\left(\boldsymbol{e}_t^{(i)}\cdot\boldsymbol{h}^{(i)}\right)}{\sum_{t'\in\mathcal{V}}\exp\left(\boldsymbol{e}_{t'}^{(i)}\cdot\boldsymbol{h}^{(i)}\right)}, \quad \mathcal{L}(\boldsymbol{\theta}^{(i)}) = \mathrm{KL}\left(p^*(t|\boldsymbol{h}^*)\middle\|p_{\boldsymbol{\theta}^{(i)}}(t|\boldsymbol{h}^{(i)})\right).$$

Since we do not update $\boldsymbol{h}^{(i)}$, the original model parameters remain unchanged, and only the newly added LM heads are trained. As demonstrated in Figure 3c, training these intermediate-layer LM heads results in good approximations of the last-layer outputs, as indicated by the low KL divergence loss at the end of training. This supports our hypothesis that intermediate-layer representations contain ample information for predicting the next token, and simple transformations via new LM heads can effectively extract this information. Consequently, with our trained LM heads, many tokens' predicted probabilities are notably high at intermediate layers, as shown in Figure 3b.

Lightweight LM head implementation. The LM heads $\boldsymbol{\theta}^{(i)} = \{\boldsymbol{e}_t^{(i)}\}_{t\in\mathcal{V}}$ are typically represented by a weight matrix $\boldsymbol{E}^{(i)} \in \mathbb{R}^{|\mathcal{V}|\times d}$ where d is the model dimension. Given the large vocabulary size of LMs, learning a separate LM head for each early prediction layer leads to a substantial increase in the number of parameters. Based on the observation that the weight matrix $\boldsymbol{E}^{(i)}$ is always applied to the hidden states $\boldsymbol{h}^{(i)}$ to compute the probability over the vocabulary $p_{\boldsymbol{\theta}^{(i)}} = \text{Softmax}(\boldsymbol{h}^{(i)}\boldsymbol{E}^{(i)\top})$, to reduce the parameter cost, we decompose it as $\boldsymbol{E}^{(i)} = \boldsymbol{E}^{*}\boldsymbol{T}^{(i)}$ where $\boldsymbol{E}^{*}$ is the last-layer LM head weights, and $\boldsymbol{T}^{(i)} \in \mathbb{R}^{d\times d}$ is a learnable transformation matrix. As $d \ll |\mathcal{V}|$ for most LLMs, learning $\boldsymbol{T}^{(i)}$ is much more parameter-efficient than learning $\boldsymbol{E}^{(i)}$ directly. We defer the proof that learning $\boldsymbol{T}^{(i)}$ retains the full expressiveness of learning $\boldsymbol{E}^{(i)}$ to Appendix C.

2.2 Parallel Token Processing via Batched Matrix Operations

Early predictions trigger parallel processing. As shown in Figure 3b, when a token's predicted probability is sufficiently high with intermediate LM heads (introduced in Section 2.1), subsequent layers are unlikely to change the predictions significantly. Based on this observation, we generate the next token t at layer $l^{(i)}$ when its probability surpasses a predefined threshold:

$$t \sim p_{\boldsymbol{\theta}^{(i)}}(t'|\boldsymbol{h}^{(i)}) \quad \text{and} \quad p_{\boldsymbol{\theta}^{(i)}}(t|\boldsymbol{h}^{(i)}) > \gamma, \tag{1}$$

where γ is a hyperparameter, and any sampling strategy can be employed (*e.g.*, greedy or nucleus sampling [25]). This allows parallel processing of the next token while completing the current token's processing. Notably, it is necessary to finish processing the remaining layers of the current token to obtain their KV cache—omitting this step would result in a missing KV cache at deeper layers, which would cause inconsistencies when computing future token representations.

Batched matrix operations for parallelization. Modern deep learning libraries (*e.g.*, PyTorch [45]) offer various approaches for parallel computation, including pipeline parallelism [30], multi-threading [13], and asynchronous execution [59]. However, our preliminary studies indicate that the actual speedups achieved by these parallelization techniques can vary widely. In many cases, these techniques do not enhance throughput and may result in longer overall decoding time, likely due to the overhead associated with scheduling, managing, and synchronizing threads and processes. Therefore, we reformulate all parallel computations as batched matrix operations to optimize hardware utilization, taking advantage of GPUs' specialization, yielding the best practical throughput. We defer the detailed implementation to Appendix B.

Early prediction verification. Regardless of the threshold hyperparameter γ set in Equation (1), there is always a possibility that the early predicted token from intermediate layers differs from the final prediction. To ensure consistency with standard autoregressive decoding, we introduce a verification step for every early prediction once the KV cache for all remaining layers has been fully computed. Specifically, we compare the early predicted token t, sampled from the intermediate layer's distribution $p_{\boldsymbol{\theta}^{(i)}}(t'|\boldsymbol{h}^{(i)})$, with the gold predicted token t^*, sampled from the final layer's distribution $p^*(t'|\boldsymbol{h}^*)$. If the two tokens do not match, we reject the early prediction:

$$\text{Reject } t \text{ if } t \neq t^*, \quad \text{where} \quad t \sim p_{\boldsymbol{\theta}^{(i)}}(t'|\boldsymbol{h}^{(i)}), \quad t^* \sim p^*(t'|\boldsymbol{h}^*).$$

When an early prediction t is rejected, we halt the generation process, replace t with the actual token t^*, and resume generation from t^* onward. Although rejecting early predictions can lead to some wasted computation, we observe in practice that this happends rarely.

3 Experiments

In this section, we focus on presenting the speedup results and hyperparameter sensitivity study, and refer readers to Appendix D for experimental details and full empirical results as well as analyses.

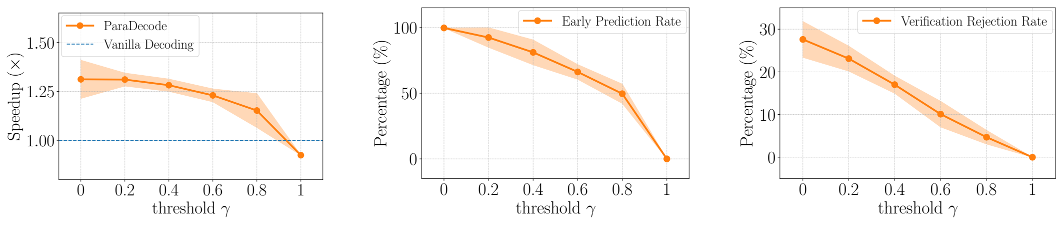

(a) Inference speedup. (b) Early prediction rate. (c) Verification rejection rate.

Figure 4: Hyperparamter study of ParaDecode by varying the early prediction threshold γ. This figure presents the evaluation results on HumanEval where (a) shows the speedup curve, (b) shows the early prediction rate, and (c) shows the verification rejection rate.

Table 1: Speedup comparison between ParaDecode and baseline decoding methods across three tasks, including text summarization, code generation, and mathematical reasoning. All compared methods ensure generation parity with vanilla autoregressive decoding, and the speedup results are computed relative to the benchmarks established on the vanilla setup (*i.e.*, speedup = $1\times$ for vanilla autoregressive decoding). '–' represents not applicable, as there is no smaller drafter from the same family of the verifier model. The best performance is highlighted in ***bold.***

Method	Text Summarization (XSum)	Code Generation (HumanEval)	Mathematical Reasoning (GSM8K)
SpecDecode [37]			
Llama3.1-8B$_{\text{INST}}$			
no smaller drafter available	–	–	–
CodeLlama-34B$_{\text{INST}}$			
w/ drafter CodeLlama-7B$_{\text{INST}}$	$1.08\times$	$1.41\times$	$1.26\times$
w/ drafter CodeLlama-13B$_{\text{INST}}$	$1.18\times$	$1.23\times$	$1.10\times$
Self-SpecDecode [57]			
Llama2-7B$_{\text{INST}}$	$1.05\times$	$1.09\times$	$1.10\times$
CodeLlama-13B$_{\text{INST}}$	$1.03\times$	$1.14\times$	$1.12\times$
CodeLlama-34B$_{\text{INST}}$	$1.07\times$	$1.14\times$	$1.14\times$
ParaDecode (Ours)			
Llama3.1-8B$_{\text{INST}}$	$1.15\times$	$1.31\times$	$1.42\times$
CodeLlama-34B$_{\text{INST}}$	**$1.24\times$**	**$1.45\times$**	**$1.53\times$**

ParaDecode can work well without searching thresholds for early predictions. As introduced in Equation (1), the hyperparameter γ controls early predictions and triggers parallel token processing. To study its impact, we implement our method with Llama3.1-8B-Instruct, and Figure 4 presents the speedup results, early prediction rate, and verification rejection rate, with varying values of $\gamma = [0, 0.2, 0.4, 0.6, 0.8, 1]$. Specifically, $\gamma = 1$ effectively means no early predictions, as very few tokens have a probability greater than 1, while $\gamma = 0$ triggers early predictions at every inference step. It can be observed that the early prediction rate decreases with increasing γ, while the verification rejection rate also decreases, and the inference speed is jointly affected by both factors. Surprisingly, we find that $\gamma = 0$ leads to the fastest overall speedup. We attribute this to the fine-tuned lightweight LM head, which enables early predictions with high confidence, suggesting that encouraging more early predictions is beneficial for speedup. This demonstrates that our method can work efficiently and accurately without hyperparameter tuning, simply by triggering early predictions at every step.

ParaDecode consistently achieves superior inference speedup across all benchmarks. To validate the effectiveness of our method, we compare the proposed ParaDecode with state-of-the-art efficient decoding methods SpecDecode and Self-SpecDecode across a wide range of challenging text generation tasks. As presented in Table 1, our method consistently delivers superior speedup compared to both SpecDecode and Self-SpecDecode in both moderate size and large size models, achieving up to $1.53\times$ speedup compared to standard autoregressive decoding.

4 Summary

In this work, we introduced ParaDecode, a new approach to accelerate autoregressive LM decoding while preserving output consistency. Empirical study shows that ParaDecode consistently achieves speedups in decoding throughput across various generation tasks compared to baselines, while requiring no auxiliary model or fine-tuning of existing model parameters. We also provide discussions on related works, limitations, and future works, which can be found in Appendices E and F.

References

[1] Josh Achiam, Steven Adler, Sandhini Agarwal, Lama Ahmad, Ilge Akkaya, Florencia Leoni Aleman, Diogo Almeida, Janko Altenschmidt, Sam Altman, Shyamal Anadkat, et al. GPT-4 technical report. *arXiv preprint arXiv:2303.08774*, 2023.

[2] Anthropic. Anthropic: Introducing claude 3.5 sonnet, 2024.

[3] Jacob Austin, Augustus Odena, Maxwell Nye, Maarten Bosma, Henryk Michalewski, David Dohan, Ellen Jiang, Carrie Cai, Michael Terry, Quoc Le, et al. Program synthesis with large language models. *arXiv preprint arXiv:2108.07732*, 2021.

[4] Jimmy Ba, Jamie Ryan Kiros, and Geoffrey E. Hinton. Layer normalization. *ArXiv*, abs/1607.06450, 2016.

[5] Sangmin Bae, Jongwoo Ko, Hwanjun Song, and Se-Young Yun. Fast and robust early-exiting framework for autoregressive language models with synchronized parallel decoding. In *Proceedings of the 2023 Conference on Empirical Methods in Natural Language Processing*, pages 5910–5924, 2023.

[6] Yushi Bai, Jiajie Zhang, Xin Lv, Linzhi Zheng, Siqi Zhu, Lei Hou, Yuxiao Dong, Jie Tang, and Juanzi Li. Longwriter: Unleashing 10,000+ word generation from long context llms. *arXiv preprint arXiv:2408.07055*, 2024.

[7] Bradley Brown, Jordan Juravsky, Ryan Ehrlich, Ronald Clark, Quoc V Le, Christopher Ré, and Azalia Mirhoseini. Large language monkeys: Scaling inference compute with repeated sampling. *arXiv preprint arXiv:2407.21787*, 2024.

[8] Tianle Cai, Yuhong Li, Zhengyang Geng, Hongwu Peng, Jason D. Lee, Deming Chen, and Tri Dao. Medusa: Simple LLM inference acceleration framework with multiple decoding heads. In *Forty-first International Conference on Machine Learning*, 2024.

[9] Charlie Chen, Sebastian Borgeaud, Geoffrey Irving, Jean-Baptiste Lespiau, Laurent Sifre, and John Jumper. Accelerating large language model decoding with speculative sampling. *arXiv preprint arXiv:2302.01318*, 2023.

[10] Mark Chen, Jerry Tworek, Heewoo Jun, Qiming Yuan, Henrique Ponde De Oliveira Pinto, Jared Kaplan, Harri Edwards, Yuri Burda, Nicholas Joseph, Greg Brockman, et al. Evaluating large language models trained on code. *arXiv preprint arXiv:2107.03374*, 2021.

[11] Karl Cobbe, Vineet Kosaraju, Mohammad Bavarian, Mark Chen, Heewoo Jun, Lukasz Kaiser, Matthias Plappert, Jerry Tworek, Jacob Hilton, Reiichiro Nakano, et al. Training verifiers to solve math word problems. *arXiv preprint arXiv:2110.14168*, 2021.

[12] Tri Dao. Flashattention-2: Faster attention with better parallelism and work partitioning. In *The Twelfth International Conference on Learning Representations*, 2024.

[13] Jeffrey Dean, Gregory S. Corrado, Rajat Monga, Kai Chen, Matthieu Devin, Quoc V. Le, Mark Z. Mao, Marc'Aurelio Ranzato, Andrew W. Senior, Paul A. Tucker, Ke Yang, and A. Ng. Large scale distributed deep networks. In *Neural Information Processing Systems*, 2012.

[14] DeepSeek. Deepseek llm: Scaling open-source language models with longtermism. *ArXiv*, abs/2401.02954, 2024.

[15] Luciano Del Corro, Allie Del Giorno, Sahaj Agarwal, Bin Yu, Ahmed Awadallah, and Subhabrata Mukherjee. Skipdecode: Autoregressive skip decoding with batching and caching for efficient llm inference. *arXiv preprint arXiv:2307.02628*, 2023.

[16] Tim Dettmers, Artidoro Pagnoni, Ari Holtzman, and Luke Zettlemoyer. QLoRA: Efficient finetuning of quantized llms. In *NeurIPS*, 2023.

[17] Alexander Yom Din, Taelin Karidi, Leshem Choshen, and Mor Geva. Jump to conclusions: Short-cutting transformers with linear transformations. *ArXiv*, abs/2303.09435, 2023.

[18] Abhimanyu Dubey, Abhinav Jauhri, Abhinav Pandey, Abhishek Kadian, Ahmad Al-Dahle, Aiesha Letman, Akhil Mathur, Alan Schelten, Amy Yang, Angela Fan, et al. The llama 3 herd of models. *arXiv preprint arXiv:2407.21783*, 2024.

[19] Maha Elbayad, Jiatao Gu, Edouard Grave, and Michael Auli. Depth-adaptive transformer. In *International Conference on Learning Representations*, 2020.

[20] Mostafa Elhoushi, Akshat Shrivastava, Diana Liskovich, Basil Hosmer, Bram Wasti, Liangzhen Lai, Anas Mahmoud, Bilge Acun, Saurabh Agarwal, Ahmed Roman, Ahmed Aly, Beidi Chen, and Carole-Jean Wu. LayerSkip: Enabling early exit inference and self-speculative decoding. In Lun-Wei Ku, Andre Martins, and Vivek Srikumar, editors, *Proceedings of the 62nd Annual Meeting of the Association for Computational Linguistics (Volume 1: Long Papers)*, pages 12622–12642, Bangkok, Thailand, August 2024. Association for Computational Linguistics.

[21] Yichao Fu, Peter Bailis, Ion Stoica, and Hao Zhang. Break the sequential dependency of LLM inference using lookahead decoding. In *Forty-first International Conference on Machine Learning*, 2024.

[22] Mor Geva, Avi Caciularu, Ke Wang, and Yoav Goldberg. Transformer feed-forward layers build predictions by promoting concepts in the vocabulary space. In *EMNLP*, 2022.

[23] Zhenyu He, Zexuan Zhong, Tianle Cai, Jason Lee, and Di He. Rest: Retrieval-based speculative decoding. In *Proceedings of the 2024 Conference of the North American Chapter of the Association for Computational Linguistics: Human Language Technologies (Volume 1: Long Papers)*, pages 1582–1595, 2024.

[24] Jordan Hoffmann, Sebastian Borgeaud, Arthur Mensch, Elena Buchatskaya, Trevor Cai, Eliza Rutherford, Diego de Las Casas, Lisa Anne Hendricks, Johannes Welbl, Aidan Clark, Tom Hennigan, Eric Noland, Katie Millican, George van den Driessche, Bogdan Damoc, Aurelia Guy, Simon Osindero, Karen Simonyan, Erich Elsen, Jack W. Rae, Oriol Vinyals, and L. Sifre. Training compute-optimal large language models. *ArXiv*, abs/2203.15556, 2022.

[25] Ari Holtzman, Jan Buys, Li Du, Maxwell Forbes, and Yejin Choi. The curious case of neural text degeneration. In *ICLR*, 2020.

[26] Coleman Hooper, Sehoon Kim, Hiva Mohammadzadeh, Hasan Genc, Kurt Keutzer, Amir Gholami, and Sophia Shao. Speed: Speculative pipelined execution for efficient decoding. *arXiv preprint arXiv:2310.12072*, 2023.

[27] Gao Huang, Danlu Chen, Tianhong Li, Felix Wu, Laurens van der Maaten, and Kilian Weinberger. Multi-scale dense networks for resource efficient image classification. In *International Conference on Learning Representations*, 2018.

[28] Kaixuan Huang, Xudong Guo, and Mengdi Wang. Specdec++: Boosting speculative decoding via adaptive candidate lengths. *arXiv preprint arXiv:2405.19715*, 2024.

[29] Lei Huang, Weijiang Yu, Weitao Ma, Weihong Zhong, Zhangyin Feng, Haotian Wang, Qianglong Chen, Weihua Peng, Xiaocheng Feng, Bing Qin, and Ting Liu. A survey on hallucination in large language models: Principles, taxonomy, challenges, and open questions. *ArXiv*, 2023.

[30] Yanping Huang, Yonglong Cheng, Dehao Chen, HyoukJoong Lee, Jiquan Ngiam, Quoc V. Le, and Z. Chen. GPipe: Efficient training of giant neural networks using pipeline parallelism. In *Neural Information Processing Systems*, 2018.

[31] Albert Q Jiang, Alexandre Sablayrolles, Antoine Roux, Arthur Mensch, Blanche Savary, Chris Bamford, Devendra Singh Chaplot, Diego de las Casas, Emma Bou Hanna, Florian Bressand, et al. Mixtral of experts. *arXiv preprint arXiv:2401.04088*, 2024.

[32] Sekitoshi Kanai, Yasuhiro Fujiwara, Yuki Yamanaka, and Shuichi Adachi. Sigsoftmax: Reanalysis of the softmax bottleneck. In *Neural Information Processing Systems*, 2018.

[33] Jared Kaplan, Sam McCandlish, Tom Henighan, Tom B Brown, Benjamin Chess, Rewon Child, Scott Gray, Alec Radford, Jeffrey Wu, and Dario Amodei. Scaling laws for neural language models. *arXiv preprint arXiv:2001.08361*, 2020.

[34] Mahsa Khoshnoodi, Vinija Jain, Mingye Gao, Malavika Srikanth, and Aman Chadha. A comprehensive survey of accelerated generation techniques in large language models. *arXiv preprint arXiv:2405.13019*, 2024.

[35] Sehoon Kim, Karttikeya Mangalam, Suhong Moon, Jitendra Malik, Michael W. Mahoney, Amir Gholami, and Kurt Keutzer. Speculative decoding with big little decoder. In *Thirty-seventh Conference on Neural Information Processing Systems*, 2023.

[36] Diederik P Kingma and Jimmy Ba. Adam: A method for stochastic optimization. *arXiv preprint arXiv:1412.6980*, 2014.

[37] Yaniv Leviathan, Matan Kalman, and Yossi Matias. Fast inference from transformers via speculative decoding. In *International Conference on Machine Learning*, pages 19274–19286. PMLR, 2023.

[38] Fangcheng Liu, Yehui Tang, Zhenhua Liu, Yunsheng Ni, Kai Han, and Yunhe Wang. Kangaroo: Lossless self-speculative decoding via double early exiting. *arXiv preprint arXiv:2404.18911*, 2024.

[39] Jiahao Liu, Qifan Wang, Jingang Wang, and Xunliang Cai. Speculative decoding via early-exiting for faster LLM inference with Thompson sampling control mechanism. In Lun-Wei Ku, Andre Martins, and Vivek Srikumar, editors, *Findings of the Association for Computational Linguistics ACL 2024*, pages 3027–3043, Bangkok, Thailand and virtual meeting, August 2024. Association for Computational Linguistics.

[40] Xiaoxuan Liu, Lanxiang Hu, Peter Bailis, Ion Stoica, Zhijie Deng, Alvin Cheung, and Hao Zhang. Online speculative decoding. *arXiv preprint arXiv:2310.07177*, 2023.

[41] Xupeng Miao, Gabriele Oliaro, Zhihao Zhang, Xinhao Cheng, Hongyi Jin, Tianqi Chen, and Zhihao Jia. Towards efficient generative large language model serving: A survey from algorithms to systems. *arXiv preprint arXiv:2312.15234*, 2023.

[42] Xupeng Miao, Gabriele Oliaro, Zhihao Zhang, Xinhao Cheng, Zeyu Wang, Zhengxin Zhang, Rae Ying Yee Wong, Alan Zhu, Lijie Yang, Xiaoxiang Shi, et al. Specinfer: Accelerating generative large language model serving with tree-based speculative inference and verification. *arXiv preprint arXiv:2305.09781*, 2023.

[43] Shashi Narayan, Shay B Cohen, and Mirella Lapata. Don't give me the details, just the summary! topic-aware convolutional neural networks for extreme summarization. In *Proceedings of the 2018 Conference on Empirical Methods in Natural Language Processing*, pages 1797–1807, 2018.

[44] OpenAI. Introducing OpenAI o1: Learning to reason with large language models, 2024.

[45] Adam Paszke, Sam Gross, Francisco Massa, Adam Lerer, James Bradbury, Gregory Chanan, Trevor Killeen, Zeming Lin, Natalia Gimelshein, Luca Antiga, Alban Desmaison, Andreas Köpf, Edward Yang, Zach DeVito, Martin Raison, Alykhan Tejani, Sasank Chilamkurthy, Benoit Steiner, Lu Fang, Junjie Bai, and Soumith Chintala. PyTorch: An imperative style, high-performance deep learning library. In *Neural Information Processing Systems*, 2019.

[46] Chau Minh Pham, Simeng Sun, and Mohit Iyyer. Suri: Multi-constraint instruction following for long-form text generation. *arXiv preprint arXiv:2406.19371*, 2024.

[47] Samyam Rajbhandari, Jeff Rasley, Olatunji Ruwase, and Yuxiong He. Zero: Memory optimizations toward training trillion parameter models. In *SC20: International Conference for High Performance Computing, Networking, Storage and Analysis*, pages 1–16. IEEE, 2020.

[48] David Raposo, Sam Ritter, Blake Richards, Timothy Lillicrap, Peter Conway Humphreys, and Adam Santoro. Mixture-of-Depths: Dynamically allocating compute in transformer-based language models. *arXiv preprint arXiv:2404.02258*, 2024.

[49] Tal Schuster, Adam Fisch, Jai Gupta, Mostafa Dehghani, Dara Bahri, Vinh Tran, Yi Tay, and Donald Metzler. Confident adaptive language modeling. *Advances in Neural Information Processing Systems*, 35:17456–17472, 2022.

[50] Charlie Snell, Jaehoon Lee, Kelvin Xu, and Aviral Kumar. Scaling llm test-time compute optimally can be more effective than scaling model parameters. *arXiv preprint arXiv:2408.03314*, 2024.

[51] Surat Teerapittayanon, Bradley McDanel, and Hsiang-Tsung Kung. Branchynet: Fast inference via early exiting from deep neural networks. In *2016 23rd international conference on pattern recognition (ICPR)*, pages 2464–2469. IEEE, 2016.

[52] Heming Xia, Zhe Yang, Qingxiu Dong, Peiyi Wang, Yongqi Li, Tao Ge, Tianyu Liu, Wenjie Li, and Zhifang Sui. Unlocking efficiency in large language model inference: A comprehensive survey of speculative decoding. *arXiv preprint arXiv:2401.07851*, 2024.

[53] Mengzhou Xia, Tianyu Gao, Zhiyuan Zeng, and Danqi Chen. Sheared LLaMA: Accelerating language model pre-training via structured pruning. In *ICLR*, 2024.

[54] Seongjun Yang, Gibbeum Lee, Jaewoong Cho, Dimitris Papailiopoulos, and Kangwook Lee. Predictive pipelined decoding: A compute-latency trade-off for exact LLM decoding. *Transactions on Machine Learning Research*, 2024.

[55] Zhilin Yang, Zihang Dai, Ruslan Salakhutdinov, and William W. Cohen. Breaking the softmax bottleneck: A high-rank RNN language model. In *ICLR*, 2018.

[56] Aohan Zeng, Xiao Liu, Zhengxiao Du, Zihan Wang, Hanyu Lai, Ming Ding, Zhuoyi Yang, Yifan Xu, Wendi Zheng, Xiao Xia, Weng Lam Tam, Zixuan Ma, Yufei Xue, Jidong Zhai, Wenguang Chen, Zhiyuan Liu, Peng Zhang, Yuxiao Dong, and Jie Tang. GLM-130b: An open bilingual pre-trained model. In *The Eleventh International Conference on Learning Representations*, 2023.

[57] Jun Zhang, Jue Wang, Huan Li, Lidan Shou, Ke Chen, Gang Chen, and Sharad Mehrotra. Draft& verify: Lossless large language model acceleration via self-speculative decoding. In Lun-Wei Ku, Andre Martins, and Vivek Srikumar, editors, *Proceedings of the 62nd Annual Meeting of the Association for Computational Linguistics (Volume 1: Long Papers)*, pages 11263–11282, Bangkok, Thailand, August 2024. Association for Computational Linguistics.

[58] Zhexin Zhang, Leqi Lei, Lindong Wu, Rui Sun, Yongkang Huang, Chong Long, Xiao Liu, Xuanyu Lei, Jie Tang, and Minlie Huang. SafetyBench: Evaluating the safety of large language models with multiple choice questions. In *ACL*, 2024.

[59] Shuxin Zheng, Qi Meng, Taifeng Wang, Wei Chen, Nenghai Yu, Zhiming Ma, and Tie-Yan Liu. Asynchronous stochastic gradient descent with delay compensation. In *ICML*, 2017.

A Overall Algorithm of ParaDecode

Algorithm 1: ParaDecode

```
Input: $\boldsymbol{x} = [x_1, x_2, \dots, x_M]$: user prompt; $\mathcal{S} = \{l^{(i)}\}\big|_{i=1}^{|\mathcal{S}|}$: early prediction layers
Parameter: $\gamma$: early prediction threshold
Output: Generated output sequence $\boldsymbol{y} = [t_0, t_1, t_2, \dots, t_N]$
KV cache $\leftarrow$ LM($\boldsymbol{x}$)                     // initialize KV cache by processing user prompt
$\boldsymbol{y} \leftarrow [t_0]$                              // initialize output sequence with BOS token
$\mathcal{P} \leftarrow \{\ \}$     // initialize a dictionary to track (token, layer) pairs being processed in parallel
$\mathcal{P}[t_0] \leftarrow 0$                                // start processing BOS token at layer 0
while $\boldsymbol{y}[-1] \neq$ EOS                           // terminate generation upon generating EOS token
 do
    update KV cache $\leftarrow$ LM($\boldsymbol{y}$; KV cache) with parallel processing of all layers in $\mathcal{P}$
    $\mathcal{P}[t] \leftarrow \mathcal{P}[t] + 1, \forall t \in \mathcal{P}$       // proceed to the next layer for all parallel layers
    if $l^{(i)} = \mathcal{P}[\boldsymbol{y}[-1]] \in \mathcal{S}$    // if the latest token $\boldsymbol{y}[-1]$ reaches an early prediction layer
     then
        $t \sim p_{\boldsymbol{\theta}^{(i)}}(t'|\boldsymbol{h}^{(i)})$                 // sample from the intermediate LM head
        if $p_{\boldsymbol{\theta}^{(i)}}(t|\boldsymbol{h}^{(i)}) > \gamma$             // if the probability surpasses the threshold
         then
            $\boldsymbol{y} \leftarrow \boldsymbol{y} \oplus t$                          // append token $t$ to output sequence
            $\mathcal{P}[t] \leftarrow 0$                              // add token $t$ at layer 0 to parallel processing
    if $\exists t \in \mathcal{P}, \mathcal{P}[t] = L$          // if any token being processed reaches the final layer $L$
     then
        $t^* \sim p^*(t'|\boldsymbol{h}^*)$                  // sample the gold token $t^*$ from final-layer predictions
        if $t^* \notin \mathcal{P}$                                  // verify early prediction if made previously
         then
            Empty $\mathcal{P}$; $\mathcal{P}[t^*] \leftarrow 0$  // reject early prediction, halt generation, and start from $t^*$ at layer 0
        remove $t$ from $\mathcal{P}$
return $\boldsymbol{y}$
```

B Detailed Design of Batched Matrix Operations for Parallelization

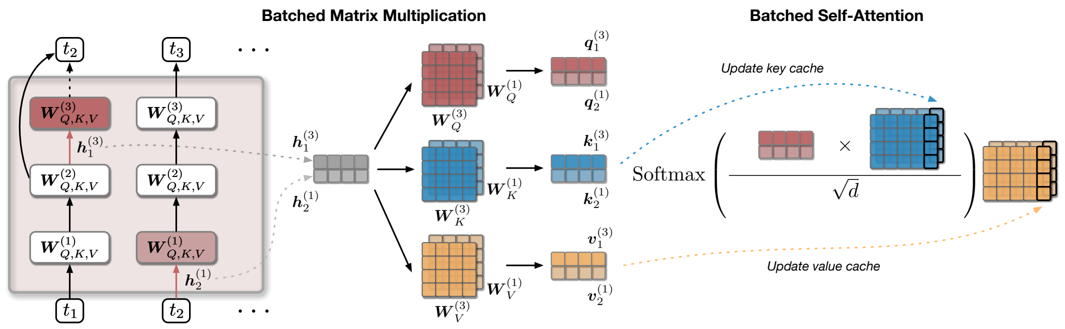

Figure 5: Parallel token processing via batched operations illustrated for the self-attention module, with other Transformer modules (*e.g.*, feedforward networks) operating similarly. If token t_2 can be generated at layer 2 while processing t_1, its computation at layer 1 starts immediately. This enables the computation of layer 1 at t_2 to run concurrently with layer 3 at t_1. Batched matrix multiplication facilitates simultaneous calculations of query, key, and value states across the parallel layers. The self-attention calculation also utilizes batched operations with updated KV cache.

Figure 5 demonstrates a specific parallel processing example: when t_2 is generated at layer 2 of t_1's processing, layer 3 computations for t_1 are executed concurrently with layer 1 computations for t_2. More generally, consider N tokens $t_1, t_2, \dots, t_N$ being processed in parallel at layers $l^{(t_1)}, l^{(t_2)}, \dots, l^{(t_N)}$ ($l^{(t_1)} < l^{(t_2)} < \cdots < l^{(t_N)}$). The corresponding input hidden states for these layers are $\boldsymbol{h}^{(t_1)}, \boldsymbol{h}^{(t_2)}, \dots, \boldsymbol{h}^{(t_N)}$. By stacking these input hidden states, we form a batched input $\boldsymbol{H}^{\oplus} = [\boldsymbol{h}^{(t_1)}; \boldsymbol{h}^{(t_2)}; \dots; \boldsymbol{h}^{(t_N)}] \in \mathbb{R}^{N \times d}$. Similarly, we prepare the batched weight matrices

$\boldsymbol{W}_X^{\oplus} = [\boldsymbol{W}_X^{(t_1)}; \boldsymbol{W}_X^{(t_2)}; \ldots; \boldsymbol{W}_X^{(t_N)}] \in \mathbb{R}^{N \times d \times d}$ where X may represent Q, K, or V. For simplicity, we assume single-head attention with $Q, K, V \in \mathbb{R}^{d \times d}$, though this approach easily generalizes to multi-head attention. The batched matrix multiplication, denoted by $\odot$ and implemented using the `torch.matmul` function, is expressed as:

$$\boldsymbol{X}^{\oplus} = \boldsymbol{H}^{\oplus} \odot \boldsymbol{W}_X^{\oplus} = \left[\boldsymbol{h}^{(t_1)} \boldsymbol{W}_X^{(t_1)}; \boldsymbol{h}^{(t_2)} \boldsymbol{W}_X^{(t_2)} \ldots; \boldsymbol{h}^{(t_N)} \boldsymbol{W}_X^{(t_N)}\right], \quad \boldsymbol{X} \in \{\boldsymbol{Q}, \boldsymbol{K}, \boldsymbol{V}\}.$$

We can then compute the self-attention outputs $\boldsymbol{O}^{\oplus}$ as follows:

$$\boldsymbol{O}^{\oplus} = \text{Softmax}\left(\frac{\boldsymbol{Q}^{\oplus} \odot \boldsymbol{K}_{\text{cache}}^{\oplus\top}}{\sqrt{d}}\right) \odot \boldsymbol{V}_{\text{cache}}^{\oplus},$$

where $\boldsymbol{K}_{\text{cache}}^{(t_i)}$ and $\boldsymbol{V}_{\text{cache}}^{(t_i)}$ denote the updated KV cache at token position t_i.

Other Transformer components, such as feedforward networks and LayerNorm [4], can also be expressed as batched matrix operations and parallelized in a similar fashion.

C Proofs

Lemma C.1. *For any $\boldsymbol{E}^{(i)} \in \mathbb{R}^{|\mathcal{V}| \times d}$, there exists a $\boldsymbol{T}^{(i)} \in \mathbb{R}^{d \times d}$ such that $\boldsymbol{E}^{(i)} = \boldsymbol{E}^* \boldsymbol{T}^{(i)}$.*

Proof. We first prove that $\boldsymbol{E}^*$ (the last-layer LM head weights) is full-rank, and then present an explicit form of $\boldsymbol{T}^{(i)}$ that satisfies $\boldsymbol{E}^{(i)} = \boldsymbol{E}^* \boldsymbol{T}^{(i)}$. During LLM pretaining, the last-layer LM head weights $\boldsymbol{E}^*$ are trained together with last layer hidden states $\boldsymbol{H}^* \in \mathbb{R}^{|\mathcal{D}| \times d}$ ($|\mathcal{D}|$ is the total number of training tokens in the corpus) to learn the ground-truth next-token prediction probability $\boldsymbol{P}^* \in \mathbb{R}^{|\mathcal{D}| \times |\mathcal{V}|}$:

$$\boldsymbol{P}^* \approx \text{Softmax}(\boldsymbol{H}^* \boldsymbol{E}^{*\top}).$$

As the softmax function cannot increase matrix rank [32], we have $\text{rank}(\text{Softmax}(\boldsymbol{H}^* \boldsymbol{E}^{*\top})) \leq \text{rank}(\boldsymbol{H}^* \boldsymbol{E}^{*\top}) \leq \min\{\text{rank}(\boldsymbol{E}^*), \text{rank}(\boldsymbol{H}^*)\} \leq \text{rank}(\boldsymbol{E}^*)$. Thus, to achieve a good approximation of $\boldsymbol{P}^*$, $\text{rank}(\boldsymbol{E}^*)$ must closely match $\text{rank}(\boldsymbol{P}^*)$. Given the complexity and diversity of natural language, the empirical distribution $\boldsymbol{P}^*$ derived from the pretraining data is extremely high-rank [55]. Therefore, to accurately model this high-rank distribution, $\boldsymbol{E}^*$ must be full-rank.

Given $\boldsymbol{E}^*$ being full-rank, $\boldsymbol{U} := \boldsymbol{E}^{*\top} \boldsymbol{E}^*$ is invertible. We can define $\boldsymbol{T}^{(i)}$ as $\boldsymbol{T}^{(i)} = \boldsymbol{U}^{-1} \boldsymbol{E}^{*\top} \boldsymbol{E}^{(i)}$, then:

$$\boldsymbol{E}^* \boldsymbol{T}^{(i)} = \boldsymbol{E}^* \boldsymbol{U}^{-1} \boldsymbol{E}^{*\top} \boldsymbol{E}^{(i)} = \left(\underbrace{\boldsymbol{E}^* (\boldsymbol{E}^{*\top} \boldsymbol{E}^*)^{-1} \boldsymbol{E}^{*\top}}_{=\boldsymbol{P}}\right) \boldsymbol{E}^{(i)}$$

Note that $\boldsymbol{P} = \boldsymbol{E}^* (\boldsymbol{E}^{*\top} \boldsymbol{E}^*)^{-1} \boldsymbol{E}^{*\top}$ is the projection matrix onto the column space of $\boldsymbol{E}^*$ (as $\boldsymbol{P}^2 = \boldsymbol{P}$). Since $\boldsymbol{E}^*$ is full rank, $\boldsymbol{E}^{(i)}$ lies in the column space of $\boldsymbol{E}^*$. Therefore, applying $\boldsymbol{P}$ to $\boldsymbol{E}^{(i)}$ gives $\boldsymbol{E}^{(i)}$ itself, confirming that $\boldsymbol{E}^{(i)}$ can be expressed as $\boldsymbol{E}^* \boldsymbol{T}^{(i)}$.

□

D Experiments

D.1 Evaluation Tasks

Evaluation tasks. We evaluate our method on a diverse set of text generation tasks, including text summarization (*i.e.*, XSum [43]), code generation (*i.e.*, HumanEval [10]), and mathematical reasoning (*i.e.*, GSM8K [11]), covering a broad spectrum of language model capabilities.

Text summarization. For text summarization, we use the widely adopted extreme summarization (XSum) dataset [43], where the models are prompted to produce a single-sentence summary of a news article, testing their ability to identify and precisely summarize the most salient information in a coherent sentence. Following previous works [57], we randomly sample 1K instances from the test split for evaluation, and 10K instances from the training split for training the lightweight LM head.

Code generation. For code generation, we evaluate our method on the HumanEval [10] benchmark, which assesses Python programming skills through a variety of coding problems, ranging from basic tasks to complex problem-solving challenges. Since the standard HumanEval benchmark does not provide a training set, we use the entire MBPP [3] dataset for training, which contains a set of crowd-sourced Python programming problems designed to be solvable by entry-level programmers, covering programming fundamentals and standard library functionality. This results in a total of 974 training samples and 164 test samples for this task.

Mathmatical reasoning. We use GSM8K [11] as the benchmark for mathematical reasoning, which contains diverse grade-school math word problems created by human problem writers. The dataset consists of 7.5K training problems and 1K test problems. These problems typically require multiple reasoning steps to solve and involve performing a sequence of basic arithmetic operations (such as addition and subtraction) to arrive at the final answer. The goal of this task is specifically to evaluate the LLM's ability in multi-step mathematical reasoning.

D.2 Baselines

In our work, we primarily focus on comparing with efficient decoding baselines that provide output parity guarantees with standard autoregressive decoding techniques, such as speculative decoding [37, 9] and self-speculative decoding [57]. Despite their conceptual advantages, these methods have practical limitations. They often come with inherent constraints regarding model selection or necessitate task-specific model architectures. For instance, speculative decoding (SpecDecode) requires the assistance of drafter models that are both smaller and derived from the same model family as the verifier model, limiting the overall flexibility in model selections. Similarly, self-speculative decoding (Self-SpecDecode) relies on a comprehensive Bayesian Optimization (BO) process to configure the model structure, allowing it to skip intermediate layers effectively for downstream tasks. Such requirements significantly compromise their practical utility and present difficulties for real-world application—as we will demonstrate later (§ D.6), they can only lead to quite limited speedup or even negative speedup results compared to standard decoding unless careful hyperparameter tuning is performed. Below, we provide a detailed introduction of the baselines.

SpecDecode. For this baseline, we consider two configurations: (1) CodeLlama-34B-Instruct as the main model (*i.e.*, verifier) with CodeLlama-13B-Instruct as the assistant model (*i.e.*, drafter), and (2) CodeLlama-34B-Instruct as the verifier with CodeLlama-7B-Instruct as the drafter. Note that it is impractical to evaluate SpecDecode with state-of-the-art moderate-sized models such as Llama3.1-8B-Instruct due to the absence of a smaller drafter model within the same family.

Self-SpecDecode. For a fair comparison, we adopt three backbone models for Self-SpecDecode: (1) Llama2-7B-chat, (2) CodeLlama-13B-Instruct, and (3) CodeLlama-34B-Instruct. Following [57], we adopt an adaptive confidence threshold strategy and set the initial threshold $\gamma^0 = 0.6$, the max number of draft token $K = 12$, and the max number of generated token $T = 512$. We run the Bayesian optimization search for 200 iterations to determine skipped layers for configuring the drafter model. We use 4 instances randomly sampled from the training set of each task for the Bayesian optimization search as suggested in the original implementation.

D.3 Implementation Details

Training details. The lightweight LM heads in our method are trained through full-parameter fine-tuning using the alignment-handbook repository[1] with Nvidia H100 GPUs. Specifically, we utilize DeepSpeed ZeRO-3 [47] along with FlashAttention [12] for distributed training, and we enable BF16 mixed precision training to enhance training efficiency. We generate on-policy data to train the lightweight LM heads by prompting the off-the-shelf Llama3.1-8B-Instruct or CodeLlama-34B-Instruct to produce responses using greedy decoding for prompts from the mixed training split obtained from the benchmarks. By default, our models are trained using the Adam optimizer [36] for 50 epochs, with a batch size of 128, a learning rate of 5e-3, and a cosine learning rate schedule with 3% warmup steps.

Inference details. During inference, we adopt the zero-shot evaluation by directly prompting the model to generate responses and apply the corresponding chat templates to format the prompts, as all backbone models used in our work are instruction-tuned versions. The framework is implemented

[1]`https://github.com/huggingface/alignment-handbook`

Table 2: Speedup comparison between ParaDecode and baseline decoding methods across three tasks, including text summarization, code generation, and mathematical reasoning. All compared methods ensure generation parity with vanilla autoregressive decoding, and the speedup results are computed relative to the benchmarks established on the vanilla setup (*i.e.*, speedup = $1\times$ for vanilla autoregressive decoding). '–' represents not applicable, as there is no smaller drafter from the same family of the verifier model. The best performance is highlighted in ***bold***.

Method	Text Summarization (XSum)	Code Generation (HumanEval)	Mathematical Reasoning (GSM8K)
SpecDecode [37]			
Llama3.1-8B$_{\text{INST}}$			
no smaller drafter available	–	–	–
CodeLlama-34B$_{\text{INST}}$			
w/ drafter CodeLlama-7B$_{\text{INST}}$	$1.08\times$	$1.41\times$	$1.26\times$
w/ drafter CodeLlama-13B$_{\text{INST}}$	$1.18\times$	$1.23\times$	$1.10\times$
Self-SpecDecode [57]			
Llama2-7B$_{\text{INST}}$	$1.05\times$	$1.09\times$	$1.10\times$
CodeLlama-13B$_{\text{INST}}$	$1.03\times$	$1.14\times$	$1.12\times$
CodeLlama-34B$_{\text{INST}}$	$1.07\times$	$1.14\times$	$1.14\times$
ParaDecode (Ours)			
Llama3.1-8B$_{\text{INST}}$	$1.15\times$	$1.31\times$	$1.42\times$
CodeLlama-34B$_{\text{INST}}$	$\mathbf{1.24}\times$	$\mathbf{1.45}\times$	$\mathbf{1.53}\times$

using the HuggingFace Transformers library[2], and we utilize the standard greedy decoding strategy as the baseline for a reproducible comparison. Following [57], the maximum number of new tokens is set to 512.

D.4 Main results

ParaDecode consistently achieves superior inference speedup across all benchmarks. To validate the effectiveness of our method, we compare the proposed ParaDecode with state-of-the-art efficient decoding methods SpecDecode and Self-SpecDecode across a wide range of challenging text generation tasks. As presented in Table 2, our method consistently delivers superior speedup compared to both SpecDecode and Self-SpecDecode in both moderate size and large size models, achieving up to $1.53\times$ speedup compared to standard autoregressive decoding.

SpecDecode (mostly) performs better when assisted with smaller models. Table 2 shows that a smaller drafter model (*e.g.*, CodeLlama-7B-Instruct) generally leads to higher speedup for SpecDecode compared to a moderate-size model (*e.g.*, CodeLlama-13B-Instruct). This is mainly because smaller drafters have fewer parameters, requiring less computation and inference time to generate draft tokens, which are then passed to a large-scale verifier (*e.g.*, CodeLlama-34B) for parallel verification and correction, significantly reducing the overall time. One notable exception is in the text summarization task, where using the smaller model as the drafter yields a lower speedup than the moderate counterpart. We speculate that this is because smaller models like CodeLlama-7B-Instruct have limited capacity to handle extremely long texts, thus producing low-quality draft tokens, which can lead to a higher rejection ratio during verification, thereby increasing the overall latency.

Self-SpecDecode tends to achieve higher speedups as the model size increases. By skipping a larger portion of intermediate layers, Self-SpecDecode can generate draft tokens much faster than the full model, thereby achieving significant speedup. However, this approach provides limited speedup improvement for mid-sized models such as Llama2-7B-Instruct. The reason is that such models have only 32 layers, skipping too many layers negatively impacts the quality of the draft tokens, which will lead to a high rejection rate during verification, and consequently increase the decoding latency. On the contrary, skipping too few layers does not yield sufficient speedup, as the performance gains stem primarily from reducing the computations associated with skipped layers.

ParaDecode guarantees output parity with standard autoregressive decoding. As shown in Table 3, we empirically evaluate the output parity guarantee of all baseline methods across three benchmarks. Despite theoretical guarantees, both SpecDecode and Self-SpecDecode fail to achieve

[2]`https://github.com/huggingface/transformers`

Table 3: Consistency ratio comparison. In principle, all compared methods in our work are expected to guarantee output parity with standard autoregressive decoding as a result of the verification steps. However, due to numerical precision inaccuracies and potentially tied probabilities during the computation, the generation results might vary in practice and are subject to experimental environment and hardware specifications. To empirically validate the output consistency of all methods with vanilla autoregressive decoding, we report the consistency ratio for all methods to ensure a fair comparison under the same experimental environment.

Method	Text Summarization (XSum)	Code Generation (HumanEval)	Mathematical Reasoning (GSM8K)
SpecDecode [37]			
CodeLlama-34B$_{\text{INST}}$			
w/ drafter CodeLlama-13B$_{\text{INST}}$	94.98%	78.56%	93.91%
Self-SpecDecode [57]			
Llama2-7B$_{\text{INST}}$	94.26%	94.83%	94.14%
CodeLlama-13B$_{\text{INST}}$	92.53%	95.20%	93.78%
CodeLlama-34B$_{\text{INST}}$	93.31%	97.79%	94.16%
ParaDecode (Ours)			
Llama3.1-8B$_{\text{INST}}$	95.36%	97.24%	95.35%
CodeLlama-34B$_{\text{INST}}$	93.27%	98.02%	94.65%

100% generation parity with standard autoregressive decoding. One possible reason is the numerical precision inaccuracies during inference, as we use BF16 precision for inference, which may cause the model to select different tokens compared to standard decoding.

D.5 Ablation Study

Table 4: Ablation study on ParaDecode. We report the performance of our method by ablating the training of the lightweight LM head and analyzing the impact of the verification step. The table shows the resulting speedup and consistency ratio on the code generation task (HumanEval).

Method	Consistency Ratio (%)	Speedup ($\times$)
ParaDecode	97.24%	1.312$\times$
w/o verification step	23.83%	1.605$\times$
w/o lightweight LM head training	71.28%	0.863$\times$

The verification step is essential for ensuring output parity. As shown in Table 4, As shown in Table 4, removing the verification step from ParaDecode significantly reduces the consistency ratio, even though it achieves a slightly higher speedup. Without verification, there is no control over the generated tokens, which can lead to ParaDecode producing entirely different content as early predictions may not always be reliable. This results in the acceptance of potentially incorrect early predicted tokens and causes significant deviations from standard autoregressive decoding. This finding underscores the importance of the verification step in our method.

Simply applying the final-layer LM head for early prediction will not lead to speedup. To validate the utility of our lightweight LM heads, we replaced the trained lightweight LM head with the final-layer LM head for early prediction. As shown in Table 4, this ablation substantially compromises the consistency ratio and, even worse, results in a negative speedup. This is because applying the final-layer LM head to intermediate layers for early prediction only produces very low confidence (as illustrated in Figure 3a), which requires frequent corrections of the early predicted tokens as few early predictions are accepted—the resultant overheads significantly slow down the decoding process because once a token is rejected, the KV cache generated during parallel computation for the next token immediately becomes invalid, as they are based on an incorrect preceding token.

D.6 Analysis

SpecDecode is sensitive to hyper-parameter configurations. Figure 6 presents the hyperparameter study for SpecDecode, indicating that it is challenging to achieve consistent speedup without careful

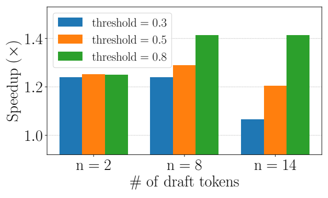

(a) SpecDec with 7B drafter.

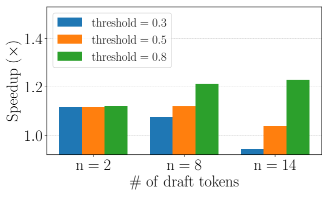

(b) SpecDec with 13B drafter.

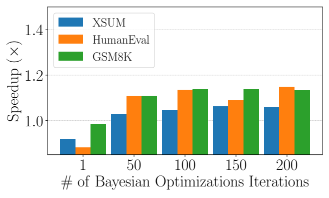

(c) Self-SpecDecode BO search.

Figure 6: Hyperparameter study of baseline models with CodeLlama-34B as the backbone model. (a) SpecDecode with CodeLlama-7B as drafter. (b) SpecDecode with CodeLlama-13B as drafter. (c) Self-SpecDecode optimized by different iterations of Bayesian optimization (BO) on three tasks.

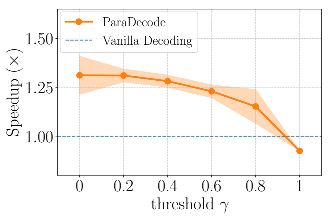

(a) Inference speedup.

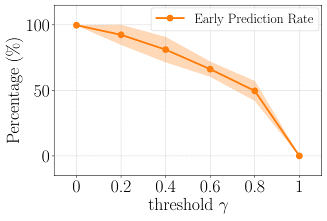

(b) Early prediction rate.

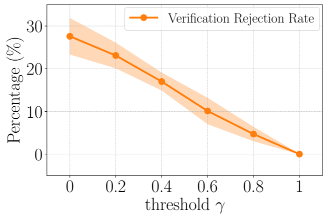

(c) Verification rejection rate

Figure 7: Hyperparamter study of ParaDecode by varying the early prediction threshold γ. This figure presents the evaluation results on HumanEval where (a) shows the speedup curve, (b) shows the early prediction rate, and (c) shows the verification rejection rate.

tuning. In this study, we use CodeLlama-34B-Instruct as the backbone model, and performed a comprehensive hyperparameter search on the HumanEval benchmark, with CodeLlama-7B-Instruct and CodeLlama-13B-Instruct as the assistant models, respectively. We explored various configurations with different max number of draft tokens n = [2, 8, 14] and confidence threshold = $[0.3, 0.5, 0.8]$. Figure 6a and Figure 6b reveal that significant speedup variance exists across different settings. Moreover, the variance becomes even larger when the confidence threshold shifts. Notably, when $n = 14$ and the threshold is 0.3, the speedup of 13B drafter is merely 0.944, which is even worse than standard decoding. These findings highlight that careful tuning hyperparameters is essential to optimize SpecDec's speedup performance and avoid potential slowdowns.

Self-SpecDecode requires task-specific architecture for optimized speedup performance. Self-SpecDecode has been proposed as a training-free, inference schema that could be employed on LMs in a plug-and-play manner. However, it requires an additional Bayesian optimization (BO) process to first obtain a set of layers to skip (as the drafter) before it can be adopted for inference. The time-consuming BO process greatly limits its practicality, moreover, it requires a set of examples as validation data to select the desired drafter. To further investigate the effect of this search process, we optimize CodeLlama-34B-Instruct with different numbers of BO iterations, as shown in Figure 6c. In general, more number of iterations could lead to improved evaluation performance. Yet, on HumanEval, it demonstrates a decrease in performance in the process. This implies scaling the number of iterations does not monotonically reflect better results, and the iteration process might require careful tuning to select an optimized drafter for inference.

ParaDecode can work well without searching thresholds for early predictions. As introduced in Equation (1), the hyperparameter γ controls early predictions and triggers parallel token processing. To study its impact, we conduct experiments with Llama3.1-8B-Instruct, and Figure 7 presents the speedup results, early prediction rate, and verification rejection rate, with varying values of $\gamma = [0, 0.2, 0.4, 0.6, 0.8, 1]$. Specifically, $\gamma = 1$ effectively means no early predictions, as very few tokens have a probability greater than 1, while $\gamma = 0$ triggers early predictions at every inference step. It can be observed that the early prediction rate decreases with increasing γ, while the verification rejection rate also decreases, and the inference speed is jointly affected by both factors. Surprisingly, we find that $\gamma = 0$ leads to the fastest overall speedup, demonstrating that our method does not require hyperparameter tuning. Based on this finding, we set $\gamma = 0$ for all experiments without further tuning, and the results in Table 2 and Table 3 confirm the effectiveness of this setting. We attribute this to the fine-tuned lightweight LM head, which enables early predictions with high confidence, resulting in a lower verification rejection rate (around 30%, as presented in Figure 7c). This finding suggests that encouraging more early predictions is beneficial for speedup and demonstrates that our method can work efficiently and accurately without hyperparameter tuning, simply by triggering early predictions at every step with the fine-tuned lightweight LM head.

E Related Work

E.1 Early Exiting

Early exiting enables language models (LMs) to complete prediction at intermediate layers, reducing computational overhead and accelerating generation. Previous approaches achieved this by adding decision branches or language modeling heads at various depths [51, 27, 19, 49]. Perhaps the most similar work to ours is [54], where the authors utilize multi-processing for pipelined decoding via early exiting. While conceptually similar, their approach diverges from ours in both method design and the implementation of parallelism—they need to train the last-layer LM head for early exiting, potentially deviating from the standard autoregressive decoding. Moreover, multi-processing incurs initialization overhead and communication costs, which also limits its practical efficiency. Another notable recent work is Mixture-of-Depth [48], which dynamically skips transformer blocks to enhance efficiency, however it still lacks the output parity guarantee with the standard autoregressive decoding. For a more detailed discussion on this line of research, we refer the readers to [34].

E.2 Speculative Decoding

Speculative decoding [37, 9] has emerged as an effective approach for speeding up language model generation. It aims to reduce decoding latency by drafting tokens using smaller auxiliary models and verifying multiple tokens in parallel with larger models, which has been actively investigated recently [23, 21, 38, 8, 39]. Among them, self-speculative decoding [57] addresses the limitation of requiring an auxiliary smaller model as the drafter. LayerSkip [20] employs early exiting to generate draft tokens while continuing with the remaining layers for verification, thereby accelerating the decoding process. Other notable works have also explored methods to handle long text sequences more efficiently [5, 35, 26]. A comprehensive overview in this area can be found in [52].

F Limitations and Future Work

Limitations. Our work focuses on accelerating LM decoding without directly improving the quality of the outputs, so ParaDecode may encounter similar issues as general LM decoding, such as hallucinations [29] and generating unsafe content [58]. Additionally, while ParaDecode consistently accelerates standard autoregressive decoding, it may occasionally incur higher FLOPs, particularly when an early-predicted token does not match the gold token, necessitating a reversion. However, such cases are rare in practice, and we find that strict parity with standard autoregressive decoding is not always necessary. The early-predicted tokens, even when they differ from the final prediction, are typically still meaningful. Therefore, one might consider relaxing strict consistency requirements to avoid unnecessary computational waste.

Future work. In the future, we plan to integrate ParaDecode with other efficiency-enhancing techniques like model pruning and quantization. Model pruning [53] offer the potential to reduce model size and parameter space by identifying and removing less critical weights or neurons. When combined with ParaDecode, pruning could lead to even faster decoding times and lower memory usage without significantly impacting performance. Similarly, ParaDecode can also be seamlessly integrated with quantization [16], which reduces the precision of model weights and activations, substantially lowering memory and compute requirements. These directions could be particularly valuable for efficient inference on mobile and edge devices.